RSC Advances

PAPER

View Article Online
View Journal | View Issue



Cite this: *RSC Adv.*, 2021, **11**, 12784

# New pentacyclic triterpenoids isolated from *Leptopus chinensis* and their hepatoprotective activities on *tert*-butyl hydroperoxide-induced oxidative injury†

Liping Long,[ab] Ye Yang,[ab] Tianliang Zhu,[ab] Xinxin Zhang,[ab] Shizhou Qi,[ab] Ting Liu,[ab] Kairu Song,[ab] Da Wang*[c] and Huiyuan Gao *[ab]

Received 4th February 2021
Accepted 8th March 2021

DOI: 10.1039/d1ra00962a

rsc.li/rsc-advances

Eight unknown pentacyclic triterpenoids (**1–4** and **8–11**), along with eight known analogues (**5–7** and **12–16**) have been first isolated from the dried whole plant of *Leptopus chinensis*. The structures of the new compounds were determined by comprehensive spectroscopic methods, including 1D and 2D NMR, as well as HRESIMS measurements. Meanwhile, the hepatoprotective activities of the isolated compounds were preliminarily evaluated, and the results indicated that compounds **2**, **5** and **16** possess potent protective effects on *tert*-butyl hydroperoxide (*t*-BHP)-induced oxidative injury *in vitro*, and further study revealed that **16** significantly alleviates *t*-BHP-induced hepatotoxicity by effectively improving cell viability and decreasing reactive oxygen species (ROS) generation and the cell apoptosis rate in HepG2 cells.



## 1. Introduction

Nowadays, multiple unfavorable life factors lead to the occurrence of various liver diseases such as fatty liver, hepatitis, liver fibrosis, liver cirrhosis and even liver cancer. These liver diseases lead to high morbidity and mortality in the public, affecting humans of all ages.[1] In China, liver diseases affect approximately 300 million people and cause a great economic burden on society.[2] During the search for new therapies to protect the liver from diverse harmful factors, natural plants have been considered as an important source to obtain potential lead compounds for the development of hepatoprotective drugs.[3,4] Furthermore, a large number of biological compounds have been isolated and glycyrrhizic acid, as well as oleanolic acid, have been used in the clinic as representative drugs from natural plants.[5,6]

Euphorbiaceae, one of the biggest families of natural plants, has been confirmed to possess significant hepatoprotective effects.[7–9] *Leptopus chinensis* (Bunge) Pojark., a perennial herbaceous plant belonging to the Euphorbiaceae family, is widely distributed in most regions of China.[10,11] This plant has been used as a type of folk medicine to treat viral hepatitis, nephritis and lung cancer.[12] However, there are no in-depth phytochemical or pharmacological investigations into this plant, and few articles have reported the presence of several triterpenoids and sterols in *L. chinensis*.[13,14] Thus, it is interesting to understand the material basis and further pharmacological effects of *L. chinensis*. As a result, eight new triterpenoids (**1–4** and **8–11**), together with eight known analogues (**5–7** and **12–16**) were obtained from the EtOAc extract of *L. chinensis* (Fig. 1). Based on the moderate hepatoprotective activity of the EtOAc fraction, these compounds were further evaluated for their hepatoprotective effect on *tert*-butyl hydroperoxide (*t*-BHP)-induced oxidative damage *in vitro*.

## 2. Experimental

### 2.1 General experimental procedures

Optical rotation values were recorded on a polarimeter (Anton-Paar MCP 200; Austria). Infrared (IR) spectra were obtained with a Fourier transform infrared spectrometer (IFS-55; Bruker). A Shimadzu UV-1700 spectrophotometer (Shimadzu, Kyoto, Japan) was used to obtain the ultraviolet (UV) spectra. The NMR spectra were recorded using ARX-400 and AV-600 spectrometers (Bruker) with TMS as an internal standard. HRESIMS data were recorded on an Agilent G6520 Q-TOF spectrometer (Santa Clara, CA, USA). Column chromatography was conducted using silica gel (100–200 mesh and 200–300 mesh, Qingdao, China) and ODS (50 μm, Aichi, Japan) as absorbents, and thin-layer chromatography (TLC) plates (GF254) were purchased from Qingdao Marine Chemical Co. Ltd. (Qingdao, China). High-performance liquid chromatography (HPLC) was performed using a Shimadzu LC-20AR instrument equipped with an SPD-20A UV detector (Shimadzu, Kyoto, Japan) and a YMC Rp-C18 column (5

[a]*School of Traditional Chinese Materia Medica, Shenyang Pharmaceutical University, Shenyang 110016, People's Republic of China. E-mail: sypugaohy@163.com*
[b]*Key Laboratory of Structure-Based Drug Design & Discovery of Ministry of Education, Shenyang Pharmaceutical University, Shenyang 110016, People's Republic of China*
[c]*School of Pharmacy, Shenyang Pharmaceutical University, Shenyang 110016, People's Republic of China*

† Electronic supplementary information (ESI) available. See DOI: 10.1039/d1ra00962a

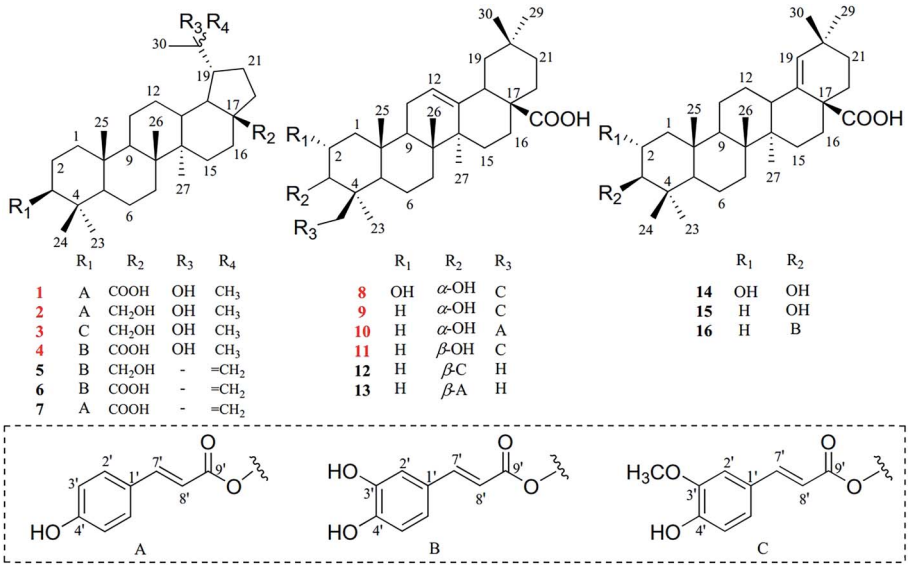


Fig. 1 Structures of compounds **1–16**.

μm, 10 × 250 mm) (YMC, Kyoto, Japan). Cell apoptosis and intracellular ROS measurements were analyzed using a Becton Dickinson FACS Calibur System. All solvents used for isolation were of analytical grade, and the reagents for HPLC were of chromatographic grade.

### 2.2 Plant material

The dried whole plant of *L. chinensis* was purchased in August 2018 from Yunnan Yuancai Biotechnology Co. Ltd. (Kunming, Yunnan, China), and it was authenticated by Associate Prof. Jiu-zhi Yuan of Shenyang Pharmaceutical University. A voucher specimen (LCH-18-08-27) was deposited in the School of Traditional Chinese Medicine, Shenyang Pharmaceutical University, Shenyang, China.

### 2.3 Extraction and isolation

The dried whole plant of *L. chinensis* (19.2 kg) was made into a powder and extracted with 75% aqueous EtOH three times under reflux. The filtered solutions were combined and evaporated under a vacuum condition to obtain a crude extract, which was suspended in water and further separated with petroleum ether, ethyl acetate and *n*-butanol, successively. The ethyl acetate extract (80.0 g) was separated using silica gel column chromatography eluted with $CH_2Cl_2$/MeOH (100 : 0 → 100 : 20) to yield fifteen fractions (Fr. 1 to Fr. 15). Fr. 3 (17.3 g) underwent further chromatography on a silica gel column and was eluted with $CH_2Cl_2$/MeOH (100 : 0 → 2 : 1) to afford six fractions (Fr. 3.1 to Fr. 3.6). Fr. 3.4 (2.0 g) was further subjected to an ODS column eluted with MeOH/$H_2O$ (40 : 60 → 95 : 5) to obtain seven more fractions (Fr. 3.4.1 to Fr. 3.4.7). Then, Fr. 3.4.3 (0.5 g) was separated by Rp-18 HPLC with MeOH/$H_2O$ (80 : 20) to obtain compounds **11** (3.0 mg, $t_R$ = 33.0 min), **12** (2.8 mg, $t_R$ = 53.5 min) and **13** (3.5 mg, $t_R$ = 41.8 min). Fr. 3.4.5 (1.5 g) was purified using semi-preparative Rp-18 HPLC with MeOH/$H_2O$ (75 : 25) to give compounds **5** (3.5 mg, $t_R$ = 126.8 min), **6** (7.2 mg, $t_R$ = 104.7 min) and **9** (5.9 mg, $t_R$ = 72.0 min). Furthermore, Fr. 3.4.6 (0.2 g) was isolated orderly by preparative and semi-preparative Rp-18 HPLC using $CH_3CN$/$H_2O$ (65 : 35) to afford compounds **3** (1.5 mg, $t_R$ = 68.3 min) and **10** (1.8 mg, $t_R$ = 37.2 min). Fr. 5 (3.0 g) was divided into six parts (Fr. 5.1 to Fr. 5.6) using an ODS column eluted with MeOH/$H_2O$ (60 : 40 → 95 : 5). Fr. 5.3 (0.5 g) was further purified by Rp-18 HPLC with MeOH/$H_2O$ (75 : 25) to yield compounds **8** (3.8 mg, $t_R$ = 63.1 min), **14** (3.2 mg, $t_R$ = 91.4 min) and **16** (5.2 mg, $t_R$ = 88.3 min), whilst Fr. 5.4 (0.3 g) was separated by Rp-18 HPLC with MeOH/$H_2O$ (80 : 20) to obtain compounds **1** (5.4 mg, $t_R$ = 84.9 min), **2** (4.5 mg, $t_R$ = 75.1 min) and **15** (2.7 mg, $t_R$ = 53.2 min). Fr. 6 (1.0 g) was first separated into six fractions (Fr. 6.1 to Fr. 6.6) using an ODS column eluted with MeOH/$H_2O$ (60 : 40 → 95 : 5), then Fr. 6.5 (0.2 g) was also isolated using HPLC with $CH_3CN$/$H_2O$ (75 : 25) to yield compounds **4** (1.7 mg, $t_R$ = 26.7 min) and **7** (3.0 mg, $t_R$ = 30.5 min).

**2.3.1 Compound 1.** 3β-*O*-*trans*-*p*-Coumaroyl-20-hydroxy-lup-28-oic acid; a white amorphous powder; $[\alpha]_D^{20}$ +1.20 (*c* 0.5, MeOH); UV (MeOH) $\lambda_{max}$ (log $\varepsilon$) 226 (3.87), 311 (4.02) nm; for $^1$H and $^{13}$C-NMR data in DMSO-$d_6$, see Table 1; HRESIMS (negative-ion mode) *m*/*z* 619.3992 $[M - H]^-$ (calc. for $C_{39}H_{55}O_6$, 619.3999).

**2.3.2 Compound 2.** 3β-*O*-*trans*-*p*-Coumaroyl-20,28-dihydroxylupane; a white amorphous powder; $[\alpha]_D^{20}$ +30.79 (*c* 0.1, MeOH); UV (MeOH) $\lambda_{max}$ (log $\varepsilon$) 227 (3.81), 311 (4.05) nm; for $^1$H and $^{13}$C-NMR data in DMSO-$d_6$, see Table 1; HRESIMS (negative-ion mode) *m*/*z* 605.4202 $[M - H]^-$ (calc. for $C_{39}H_{57}O_5$, 605.4206).

**2.3.3 Compound 3.** 3β-*O*-*trans*-Feruloyl-20,28-dihydroxylupane; a white amorphous powder; $[\alpha]_D^{20}$ +7.04 (*c* 0.4, MeOH); UV (MeOH) $\lambda_{max}$ (log $\varepsilon$) 232 (3.96), 324 (4.01) nm; for $^1$H and $^{13}$C-NMR data in $CDCl_3$, see Table 1; HRESIMS (negative-ion mode) *m*/*z* 635.4321 $[M - H]^-$ (calc. for $C_{40}H_{59}O_6$, 635.4312).

**2.3.4 Compound 4.** 3β-*O*-*trans*-Caffeoyl-20-hydroxy-lup-28-oic acid; a white amorphous powder; $[\alpha]_D^{20}$ +5.8 (*c* 0.5, MeOH);

Table 1 The NMR data of compounds 1–4

| | 1 | | 2 | | 3 | | 4 | |
|---|---|---|---|---|---|---|---|---|
| No. | $\delta_H$[a] $J$ (Hz) | $\delta_C$[b] | $\delta_H$[a] $J$ (Hz) | $\delta_C$[b] | $\delta_H$[c] $J$ (Hz) | $\delta_C$[d] | $\delta_H$[a] $J$ (Hz) | $\delta_C$[b] |
| 1 | 1.69 o, 1.01 m | 37.9 | 1.67 o, 0.99 m | 38.4 | 1.70 o, 1.04 m | 38.5 | 1.69 o, 0.99 m | 37.9 |
| 2 | 1.66 o, 1.58 m | 23.5 | 1.72 o, 1.30 m | 27.9 | 1.83 o, 0.93 m | 29.1 | 1.64 o, 1.58 m | 23.5 |
| 3 | 4.50 dd (11.6, 4.6) | 79.8 | 4.50 dd (11.4, 4.6) | 80.3 | 4.62 dd (11.2, 4.9) | 80.9 | 4.49 dd (11.6, 4.5) | 79.8 |
| 4 | — | 40.1 | — | 38.1 | — | 38.2 | — | 40.1 |
| 5 | 0.85 o | 54.6 | 0.85 o | 55.0 | 0.84 o | 55.4 | 0.85 o | 54.6 |
| 6 | 1.47 m, 1.38 o | 17.8 | 1.48 m, 1.40 o | 18.3 | 1.53 m, 1.41 o | 18.4 | 1.47 m, 1.38 o | 17.8 |
| 7 | 1.38 o, 1.34 m | 34.1 | 1.54 m, 1.41 o | 36.4 | 1.42 o, 1.04 m | 34.6 | 1.38 o, 1.33 m | 34.1 |
| 8 | — | 40.7 | — | 41.5 | — | 41.6 | — | 40.7 |
| 9 | 1.30 o | 49.8 | 1.31 o | 50.1 | 1.31 o | 50.3 | 1.31 o | 49.8 |
| 10 | — | 36.6 | — | 37.0 | — | 37.2 | — | 36.6 |
| 11 | 1.42 o, 1.15 m | 21.2 | 2.04 o, 0.88 o | 28.4 | 1.90 o, 1.39 m | 28.4 | 1.43 m, 1.16 m | 21.2 |
| 12 | 1.67 o, 1.45 m | 28.2 | 1.03 m, 0.92 m | 27.4 | 1.78 m, 1.07 m | 27.3 | 1.68 o, 1.45 m | 28.2 |
| 13 | 2.26 td (12.7, 3.3) | 37.6 | 1.39 o | 34.4 | 1.63 o | 36.3 | 2.26 td (12.6, 3.6) | 37.6 |
| 14 | — | 42.8 | — | 43.4 | — | 43.5 | — | 42.8 |
| 15 | 1.46 m, 1.07 m | 29.6 | 1.76 m, 0.72 m | 33.5 | 1.91 o, 1.80 m | 33.5 | 1.46 m, 1.10 m | 29.6 |
| 16 | 2.12 td (12.2, 3.2) | 31.9 | 1.86 dt (10.7, 2.0) | 30.1 | 1.92 o | 29.9 | 2.12 dd (12.2, 3.0) | 31.9 |
| | 1.32 o | | 1.05 o | | 1.25 o | | 1.31 o | |
| 17 | — | 57.9 | — | 49.0 | — | 49.3 | — | 57.9 |
| 18 | 1.48 o | 47.8 | 1.40 o | 48.6 | 1.56 o | 48.9 | 1.48 o | 47.8 |
| 19 | 2.01 td (10.5, 2.1) | 48.8 | 1.69 o | 50.2 | 1.83 o | 49.9 | 2.01 td (9.3, 1.8) | 48.8 |
| 20 | — | 71.3 | — | 71.8 | — | 73.7 | — | 71.3 |
| 21 | 1.75 o, 1.24 m | 28.5 | 1.65 o, 1.59 m | 24.0 | 1.69 o, 1.64 m | 24.0 | 1.75 o, 1.24 m | 28.5 |
| 22 | 1.59 m, 1.29 m | 36.2 | 1.39 m, 1.16 m | 21.4 | 1.49 m, 1.25 m | 21.5 | 1.60 m, 1.29 m | 36.2 |
| 23 | 0.82 s | 27.7 | 0.82 s | 28.2 | 0.90 s | 28.2 | 0.82 s | 27.7 |
| 24 | 0.87 s | 16.1 | 0.88 s | 17.1 | 0.92 s | 16.8 | 0.87 s | 16.1 |
| 25 | 0.84 s | 16.0 | 0.85 s | 16.4 | 0.89 s | 16.4 | 0.84 s | 16.0 |
| 26 | 0.88 s | 16.6 | 1.01 s | 16.3 | 1.00 s | 16.3 | 0.88 s | 16.6 |
| 27 | 0.96 s | 14.8 | 0.95 s | 15.5 | 1.06 s | 15.2 | 0.96 s | 14.8 |
| 28 | — | 177.7 | 3.57 dd (10.4, 5.4) | 58.9 | 3.86 d (10.8) | 61.0 | — | 177.7 |
| | | | 3.04 dd (10.4, 5.4) | | 3.32 d (10.8) | | | |
| 29 | 1.08 s | 31.0 | 1.09 s | 32.2 | 1.14 s | 31.8 | 1.08 s | 30.9 |
| 30 | 1.00 s | 26.3 | 0.98 s | 25.4 | 1.24 s | 24.8 | 0.99 s | 26.3 |
| 1′ | — | 125.1 | — | 125.6 | — | 127.3 | — | 125.5 |
| 2′ | 7.54 d (8.6) | 130.3 | 7.54 d (8.6) | 130.8 | 7.03 d (1.8) | 109.4 | 7.03 d (1.8) | 114.8 |
| 3′ | 6.78 d (8.6) | 115.8 | 6.78 d (8.6) | 116.2 | — | 146.9 | — | 145.6 |
| 4′ | — | 159.8 | — | 160.2 | — | 148.0 | — | 148.3 |
| 5′ | 6.78 d (8.6) | 115.8 | 6.78 d (8.6) | 116.2 | 6.91 d (8.2) | 114.8 | 6.75 d (8.2) | 115.7 |
| 6′ | 7.54 d (8.6) | 130.3 | 7.54 d (8.6) | 130.8 | 7.07 dd (8.2, 1.8) | 123.2 | 6.99 dd (8.2, 1.8) | 121.3 |
| 7′ | 7.53 d (16.0) | 144.4 | 7.52 d (16.0) | 144.9 | 7.59 d (15.9) | 144.5 | 7.44 d (15.9) | 144.8 |
| 8′ | 6.36 d (16.0) | 114.6 | 6.36 d (16.0) | 115.1 | 6.29 d (15.9) | 116.4 | 6.23 d (15.9) | 114.3 |
| 9′ | — | 166.4 | — | 166.8 | — | 167.3 | — | 166.3 |
| 3′-$OCH_3$ | — | — | — | — | 3.93 s | 56.1 | — | — |
| 28-COOH | 11.88 brs | — | — | — | — | — | 11.97 brs | — |

[a] Recorded at 600 MHz in DMSO-$d_6$. [b] Recorded at 150 MHz in DMSO-$d_6$. [c] Recorded at 600 MHz in $CDCl_3$. [d] Recorded at 150 MHz in $CDCl_3$ ("o" overlapped).

UV (MeOH) $\lambda_{max}$ (log $\varepsilon$) 218 (3.85), 320 (4.03) nm; for $^1$H and $^{13}$C-NMR data in DMSO-$d_6$, see Table 1; HRESIMS (negative-ion mode) $m/z$ 635.3942 $[M - H]^-$ (calc. for $C_{39}H_{55}O_7$, 635.3948).

**2.3.5 Compound 8.** 24-*O*-*trans*-Feruloyl-2α,3α-dihydroxy-olean-12-en-28-oic acid; a white amorphous powder; $[\alpha]_D^{20}$ +16.36 (*c* 0.4, MeOH); UV (MeOH) $\lambda_{max}$ (log $\varepsilon$) 230 (3.93), 325 (3.90) nm; for $^1$H and $^{13}$C-NMR data in DMSO-$d_6$, see Table 2; HRESIMS (negative-ion mode) $m/z$ 663.3891 $[M - H]^-$ (calc. for $C_{40}H_{55}O_8$, 663.3897).

**2.3.6 Compound 9.** 24-*O*-*trans*-Feruloyl-3α-hydroxy-olean-12-en-28-oic acid; a white amorphous powder; $[\alpha]_D^{20}$ +16.60 (*c* 0.5, MeOH); UV (MeOH) $\lambda_{max}$ (log $\varepsilon$) 235 (3.85), 325 (3.91) nm; for $^1$H and $^{13}$C-NMR data in DMSO-$d_6$, see Table 2; HRESIMS (negative-ion mode) $m/z$ 647.3955 $[M - H]^-$ (calc. for $C_{40}H_{55}O_7$, 647.3948).

**2.3.7 Compound 10.** 24-*O*-*trans*-*p*-Coumaroyl-3α-hydroxy-olean-12-en-28-oic acid; a white amorphous powder; $[\alpha]_D^{20}$ +13.6 (*c* 0.5, MeOH); UV (MeOH) $\lambda_{max}$ (log $\varepsilon$) 225 (3.84), 312 (3.91) nm; for $^1$H and $^{13}$C-NMR data in DMSO-$d_6$, see Table 2; HRESIMS (negative-ion mode) $m/z$ 617.3837 $[M - H]^-$ (calc. for $C_{39}H_{53}O_6$, 617.3842).

**2.3.8 Compound 11.** 24-*O*-*trans*-Feruloyl-3β-hydroxy-olean-12-en-28-oic acid; a white amorphous powder; $[\alpha]_D^{20}$ +49.0 (*c*

 

Table 2 The NMR data of compounds 8–11

| | 8 | | 9 | | 10 | | 11 | |
|---|---|---|---|---|---|---|---|---|
| No. | $\delta_H$[a] $J$ (Hz) | $\delta_C$[b] | $\delta_H$[a] $J$ (Hz) | $\delta_C$[b] | $\delta_H$[a] $J$ (Hz) | $\delta_C$[b] | $\delta_H$[a] $J$ (Hz) | $\delta_C$[b] |
| 1 | 1.41 o, 1.18 o | 41.4 | 1.33 m, 1.14 m | 32.8 | 1.33 m, 1.13 m | 32.8 | 1.56 o, 0.97 m | 38.1 |
| 2 | 3.77 o | 64.4 | 1.83 o, 1.43 m | 25.0 | 1.83 o, 1.42 m | 25.0 | 1.56 o, 1.51 m | 26.9 |
| 3 | 3.50 dd (6.1, 2.8) | 72.7 | 3.52 dd (6.3, 2.7) | 68.5 | 3.51 dd (6.4, 2.5) | 68.5 | 3.16 dd (11.8, 4.9) | 76.9 |
| 4 | — | 42.5 | — | 41.3 | — | 41.3 | — | 41.6 |
| 5 | 1.31 o | 48.2 | 1.38 o | 48.8 | 1.38 o | 48.8 | 0.84 o | 55.0 |
| 6 | 1.50 m, 1.32 m | 17.9 | 1.50 m, 1.39 m | 18.0 | 1.50 m, 1.38 m | 18.0 | 1.71 o, 1.52 o | 19.5 |
| 7 | 1.86 o, 1.23 m | 32.6 | 1.43 m, 1.23 m | 32.6 | 1.42 m, 1.26 m | 32.6 | 1.36 m, 1.27 m | 33.0 |
| 8 | — | 39.0 | — | 39.0 | — | 39.0 | — | 38.9 |
| 9 | 1.61 o | 47.1 | 1.62 o | 47.0 | 1.62 o | 47.0 | 1.52 o | 47.2 |
| 10 | — | 37.6 | — | 36.5 | — | 36.5 | — | 36.6 |
| 11 | 1.85 o, 0.88 o | 23.1 | 1.84 o, 1.62 o | 23.0 | 1.84 o, 1.62 o | 23.0 | 1.82 o, 1.01 m | 23.0 |
| 12 | 5.18 brt (3.2) | 121.4 | 5.18 brt (3.4) | 121.5 | 5.17 brt (3.3) | 121.5 | 5.17 brt (3.4) | 121.5 |
| 13 | — | 143.9 | — | 143.8 | — | 143.8 | — | 143.8 |
| 14 | — | 41.3 | — | 41.2 | — | 41.2 | — | 41.3 |
| 15 | 1.66 m, 0.99 o | 27.1 | 1.65 o, 0.99 o | 27.1 | 1.65 o, 1.01 o | 27.1 | 1.63 o, 0.99 o | 27.2 |
| 16 | 1.91 td (13.5, 3.7) | 22.6 | 1.92 td (13.4, 3.7) | 22.7 | 1.92 td (13.3, 3.4) | 22.7 | 1.91 td (13.4, 3.7) | 22.6 |
| | 1.48 o | | 1.48 o | | 1.49 o | | 1.48 o | |
| 17 | — | 45.4 | — | 45.4 | — | 45.4 | — | 45.5 |
| 18 | 2.75 dd (13.2, 4.0) | 40.7 | 2.75 dd (13.2, 4.0) | 40.8 | 2.75 dd (13.8, 4.1) | 40.8 | 2.74 dd (13.7, 4.0) | 40.8 |
| 19 | 1.61 o, 1.06 m | 45.7 | 1.62 o, 1.05 m | 45.7 | 1.62 o, 1.07 m | 45.7 | 1.62 o, 1.06 m | 45.7 |
| 20 | — | 30.4 | — | 30.4 | — | 30.4 | — | 30.4 |
| 21 | 1.33 m, 1.13 m | 33.3 | 1.33 m, 1.14 m | 33.3 | 1.32 m, 1.15 m | 33.3 | 1.32 m, 1.14 m | 33.3 |
| 22 | 1.61 o, 1.44 m | 32.1 | 1.60 o, 1.43 m | 32.1 | 1.61 o, 1.45 m | 32.1 | 1.61 o, 1.44 m | 32.1 |
| 23 | 1.04 s | 22.9 | 0.99 s | 22.6 | 0.98 s | 22.6 | 1.09 s | 22.8 |
| 24 | 4.26 d (11.4) | 66.4 | 4.27 d (11.3) | 66.8 | 4.26 d (11.3) | 66.8 | 4.24 d (11.7) | 65.8 |
| | 3.96 d (11.4) | | 3.98 d (11.3) | | 3.97 d (11.3) | | 4.19 d (11.7) | |
| 25 | 0.92 s | 16.4 | 0.88 s | 15.2 | 0.88 s | 15.2 | 0.89 s | 14.8 |
| 26 | 0.70 s | 16.7 | 0.70 s | 16.7 | 0.71 s | 16.7 | 0.71 s | 16.6 |
| 27 | 1.11 s | 25.7 | 1.12 s | 25.7 | 1.12 s | 25.7 | 1.10 s | 25.5 |
| 28 | — | 178.6 | — | 178.6 | — | 178.6 | — | 178.6 |
| 29 | 0.88 s | 32.8 | 0.89 s | 32.7 | 0.88 s | 32.7 | 0.87 s | 32.8 |
| 30 | 0.88 s | 23.4 | 0.88 s | 23.4 | 0.88 s | 23.4 | 0.87 s | 23.4 |
| 1′ | — | 125.5 | — | 125.5 | — | 125.0 | — | 125.6 |
| 2′ | 7.31 d (1.7) | 111.2 | 7.31 d (1.8) | 111.2 | 7.54 d (8.6) | 130.3 | 7.28 d (1.8) | 111.2 |
| 3′ | — | 148.0 | — | 148.0 | 6.79 d (8.6) | 115.8 | — | 148.0 |
| 4′ | — | 149.4 | — | 149.3 | — | 159.8 | — | 149.3 |
| 5′ | 6.79 d (8.2) | 115.5 | 6.79 d (8.2) | 115.5 | 6.79 d (8.6) | 115.8 | 6.80 d (8.2) | 115.6 |
| 6′ | 7.11 dd (8.2, 1.7) | 123.2 | 7.10 dd (8.2, 1.8) | 123.2 | 6.79 d (8.6) | 130.3 | 7.08 dd (8.2, 1.8) | 123.1 |
| 7′ | 7.52 d (15.9) | 145.0 | 7.52 d (15.9) | 145.0 | 7.52 d (15.9) | 144.6 | 7.51 d (15.9) | 144.6 |
| 8′ | 6.45 d (15.9) | 114.5 | 6.44 d (15.9) | 114.6 | 6.36 d (15.9) | 114.2 | 6.40 d (15.9) | 115.0 |
| 9′ | — | 166.7 | — | 166.8 | — | 166.7 | — | 166.9 |
| 3′-$OCH_3$ | 3.82 s | — | 3.82 s | 55.7 | — | — | 3.82 s | 55.8 |
| 28-COOH | 12.04 brs | — | 12.03 brs | — | 12.03 brs | — | 11.96 brs | — |

[a] Recorded at 600 MHz in DMSO-$d_6$. [b] Recorded at 150 MHz in DMSO-$d_6$ ("o" overlapped).

0.5, MeOH); UV (MeOH) $\lambda_{max}$ (log $\varepsilon$) 236 (3.88), 320 (3.90) nm; for $^1$H and $^{13}$C-NMR data in DMSO-$d_6$, see Table 2; HRESIMS (negative-ion mode) $m/z$ 647.3942 $[M - H]^-$ (calc. for $C_{40}H_{55}O_7$, 647.3948).

### 2.4 Cell culture

HepG2 cells were purchased from the Stem Cell Bank, Chinese Academy of Science, China. The cells were cultured in DMEM medium (Gibco, USA), supplemented with 10% fetal bovine serum (Gibco, USA) and 0.5% penicillin/streptomycin in a humidified atmosphere of 5% $CO_2$ at 37 °C.

### 2.5 Evaluation of hepatoprotective activity

The hepatoprotective activities of isolated compounds were measured using the MTT method. Briefly, the cells in the logarithmic growth phase were incubated in 96-well flat-bottomed cell culture at a density of $5 \times 10^3$ cells per well and were cultured overnight, before being pretreated with isolated compounds and a positive control (silymarin and ammonium glycyrrhetate) that was diluted to a specified concentration for 2 h. $t$-BHP was then added to a final concentration of 1 mM and the solutions were incubated for 2.5 h. Afterwards, MTT solution (5 mg $mL^{-1}$) was added to each well and the solutions

were incubated for another 3 h. The supernatant was removed, and the deposited formazan crystals were dissolved with DMSO, followed by the plates being shaken mildly to blend the mixture. The optical densities at 490 nm were measured using a Varioskan Flash Multimode Reader (Thermo Scientific). All experiments were performed at least three times.

### 2.6 Intracellular ROS measurements

A DCFH-DA fluorescent probe was used for assessing the intracellular ROS production. Briefly, HepG2 cells were seeded in 6-well plates at a density of $4 \times 10^5$ cells per well overnight, and the plates were then incubated with DCFH-DA (10 μM) at 37 °C for 30 min and washed three times with PBS. Next, the cells were pretreated with different concentrations of compound **16** for 2 h, and were subsequently exposed to *t*-BHP (1 mM) for an additional 1 h. Cells were collected for analysis with laser scanning confocal microscopy and flow cytometry.

### 2.7 Apoptosis assay

**2.7.1 Hoechst 33258 staining assay.** The Hoechst 33258 fluorescent dye was employed to analyze the nuclei morphology, as described previously.[15] Briefly, HepG2 cells were seeded in 24-well plates at a density of $5 \times 10^4$ cells per well overnight, and the cells were then pretreated with different concentrations of compound **16** for 2 h, followed by exposure to *t*-BHP (1 mM) for an additional 1 h. Next, the cells were fixed with paraformaldehyde for 10 min, stained with Hoechst 33258 (10 μg $mL^{-1}$) for 5 min and observed using a laser scanning confocal microscope.

**2.7.2 Annexin V-FITC/PI double staining.** Annexin V-FITC/PI double staining was used to analyze cell apoptosis, as described previously.[16] HepG2 cells were seeded in 6-well plates at a density of $4 \times 10^5$ cells per well overnight, and they were then pretreated with compound **16** at different concentrations for 2 h, followed by exposure to *t*-BHP (1 mM) for an additional 1.5 h. Finally, the cells were collected and washed with ice-cold PBS, and the percentages of apoptosis and necrosis were determined with FITC-labeled annexin V and propidium iodide staining using flow cytometry.

### 2.8 Statistical analysis

The results were expressed as mean values ± standard deviation. A one-way ANOVA test was used to evaluate the differences between the means of the groups using SPSS 19.0 software, and a $p$ value less than 0.05 was considered to be significantly different.

## 3. Results and discussion

### 3.1 Structure elucidation

Compound **1** was obtained as a white amorphous powder and the molecular formula of $C_{39}H_{56}O_6$ was deduced from HRESIMS data at $m/z$ 619.3992 $[M - H]^-$ (calc. for $C_{39}H_{55}O_6$, 619.3999) and NMR data (Table 1). The $^1$H-NMR data of **1** showed signals of seven tertiary methyl singlets at $\delta_H$ 1.08, 1.00, 0.96, 0.88, 0.87, 0.84, and 0.82, as well as an oxygenated methine at $\delta_H$ 4.50 (dd, 11.6, 4.6 Hz, H-3). Moreover, the signals of two olefinic protons at $\delta_H$ 7.53 and 6.36 (each a d, 16.0 Hz, H-7′, 8′), and an aromatic proton spin system at $\delta_H$ 7.54 (d, 8.6 Hz, H-2′, 6′) and $\delta_H$ 6.78 (d, 8.6 Hz, H-3′, 5′) indicated the presence of a *trans-p*-coumaroyl unit. 39 Carbon signals were observed in the $^{13}$C-NMR (Table 1), including two carbonyl groups at $\delta_C$ 177.7 (C-28) and 166.4 (C-9′), a 1,4-disubstituted aromatic system at $\delta_C$ 159.8 (C-4′), 130.3 (C-2′, 6′), 125.1 (C-1′), and 115.8 (C-3′, 5′), two olefinic carbons at $\delta_C$ 144.4 (C-7′) and 114.6 (C-8′), and two oxygenated aliphatic signals at $\delta_C$ 79.8 (C-3) and 71.3 (C-20). Based on the 1D NMR, HSQC and HMBC data, compound **1** can be assigned as a triterpenoid skeleton linked with a *trans-p*-coumaroyl unit. Comparison of its 1D NMR data with the data of 3β-*O-trans*-coumaroyl betulinic acid indicated that they have a similar lupane-type triterpenoid skeleton,[17] except for the presence of a hydroxyl unit at C-20 in **1**. The key HMBC correlations of H-29/C-20, H-30/C-20, OH-20/C-20, and OH-20/C-30, combined with the signals of the double band unit, were not detected in the $^{13}$C-NMR spectrum, suggesting the connection of the hydroxyl unit to C-20. In addition, the correlation (Fig. 2A) of H-3 to C-9′ showed that the *O-trans-p*-coumaroyl moiety was attached to C-3 of the lupane framework. Furthermore, the NOESY correlations (Fig. 2B) from H-3 to H-5 and H-9, and the coupling constant of $J_{H\text{-}2\beta/H\text{-}3\alpha} = 11.2$ Hz, showed that H-3 is α-oriented. In conclusion, the structure of compound **1** was defined as 3β-*O-trans-p*-coumaroyl-20-hydroxy-lup-28-oic acid.

Compounds **2** and **3** were isolated as white amorphous powders, and their molecular formulas were identified from the HRESIMS data at $m/z$ 605.4202 $[M - H]^-$ (calc. for $C_{39}H_{57}O_5$, 605.4206) and 635.4321 $[M - H]^-$ (calc. for $C_{40}H_{59}O_6$, 635.4312), respectively. The NMR spectrum of **2** was almost identical to that of **1** and suggested that the 28-carboxyl group present in **1** was replaced by a hydroxymethyl group in **2**, and this was deduced from the proton signals of two oxygenated methylene groups at $\delta_H$ 3.57 and 3.04 (each a dd, 10.4, 5.4 Hz, H-28α, 28β) and the HMBC correlations (Fig. 2A) of H-28α and H-28β to C-16 ($\delta_C$ 30.1). Additionally, a comparison of the NMR data of **3** with that of **2** showed that the spectra were very similar, except for the presence of a *trans*-feruloyl unit in **3** rather than a *trans-p*-coumaroyl moiety in **2**. On the basis of the HRESIMS and 1D NMR spectroscopic data, the *trans*-feruloyl moiety was identified from the proton signals at $\delta_H$ 7.07 (dd, 8.2, 1.8 Hz, H-6′), 7.03 (d, 1.8 Hz, H-2′) 6.91 (d, 8.2 Hz, H-5′) and 3.93 (s, 3′-$OCH_3$), in accordance with the two oxygenated aromatic carbon signals at $\delta_C$ 146.9 (C-3′) and 148.0 (C-4′), and a methoxy signal at $\delta_C$ 56.1 (3′-$OCH_3$). In addition, the HMBC spectra (Fig. 2A) of compounds **2** and **3** showed the key correlation from H-3 to C-9′, and the coupling constants of $J_{H\text{-}2\beta/H\text{-}3\alpha}$ and NOESY correlations were identical to those of **1**. Consequently, the structures of **2** and **3** were elucidated as 3β-*O-trans-p*-coumaroyl-20,28-dihydroxy-lupane and 3β-*O-trans*-feruloyl-20,28-dihydroxylupane, respectively.

Compound **4** was purified as a white amorphous powder with the molecular formula of $C_{39}H_{56}O_7$, as determined by negative mode HRESIMS data at $m/z$ 635.3942 ($[M - H]^-$, calc. as 635.3948). According to its 1D NMR (Table 1), HSQC and HMBC data, **4** was found to show quite similar results to **1**, with the main difference between them being that the *trans-p*-coumaroyl group of **1** was replaced with the *trans*-caffeoyl group of **4**. This conclusion

 

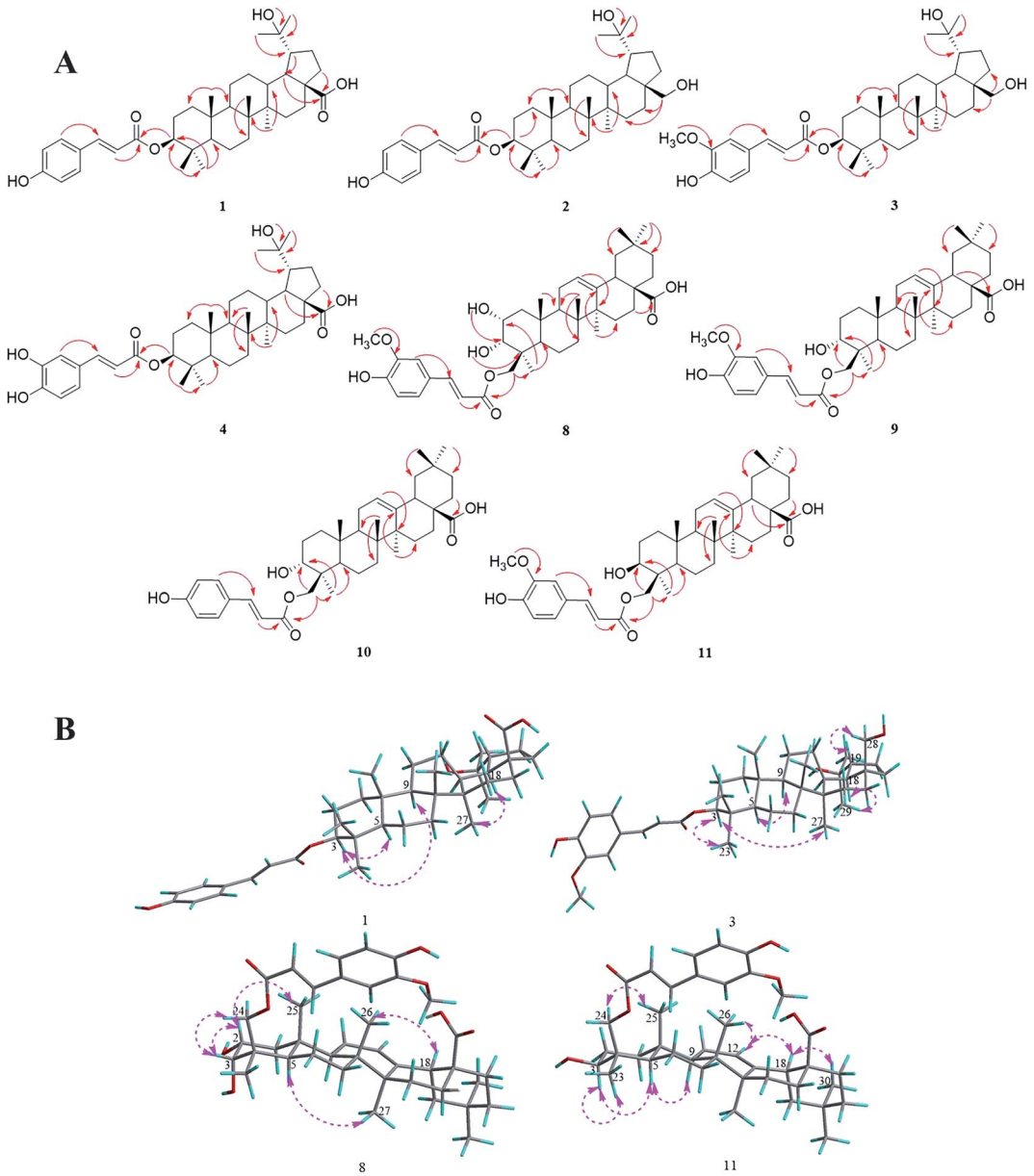


Fig. 2 (A) Key HMBC correlations of compounds **1–4** and **8–11**. (B) Major NOESY correlations within compounds **1**, **3**, **8** and **11**.

could be verified by the signals of a 1,3,4-trisubstituted aromatic proton spin system at $\delta_H$ 7.03 (d, 1.8 Hz, H-2′), 6.99 (dd, 8.2, 1.8 Hz, H-6′) and 6.75 (d, 8.2 Hz, H-5′), along with the two oxygenated aromatic carbon signals at $\delta_C$ 148.3 (C-4′) and 145.6 (C-3′). Moreover, the key HMBC correlation (Fig. 2A) from H-3 to C-9' ($\delta_C$ 166.3) indicated that an *O-trans*-caffeoyl moiety was located at C-3, and the NOESY correlations showed that **4** has the same relative configuration as **1**. Thus, compound **4** was elucidated as 3β-*O-trans*-caffeoyl-20-hydroxy-lup-28-oic-acid.

Compound **8** was obtained as a white amorphous powder, and its molecular formula was identified as $C_{40}H_{56}O_8$ on the basis of the 1D NMR and HRESIMS data with an $[M-H]^-$ ion at *m*/*z* 663.3891 (calc. for $C_{40}H_{55}O_8$, 663.3897). The $^1$H-NMR spectrum (Table 2) of compound **8** showed proton signals of six tertiary methyl singlets at $\delta_H$ 0.70, 0.88, 0.88, 0.92, 1.04, and 1.11, one olefinic proton at $\delta_H$ 5.18 (brt, 3.2 Hz, H-12) and two oxygenated methines at $\delta_H$ 3.77 (overlap, H-2) and 3.50 (dd, 6.1, 2.8 Hz, H-3). Moreover, the *trans*-feruloyl unit was determined based on the signals of an aromatic proton spin system at $\delta_H$ 7.31 (d, 1.7 Hz, H-2′), 7.11 (dd, 8.2, 1.7 Hz, H-6′) and 6.79 (d, 8.2 Hz, H-5′), a double bond at $\delta_H$ 7.52 and 6.45 (each a d, 15.9 Hz, H-7′, 8′) and a methoxy singlet at $\delta_H$ 3.82 (s, 3′-$OCH_3$). The $^{13}$C-NMR data (Table 2) revealed the occurrence of 40 carbon signals, including one double bond at $\delta_C$ 121.4 (C-11) and 143.9 (C-12), three oxygenated aliphatic carbons at $\delta_C$ 72.7 (C-3), 66.4 (C-24) and 64.4 (C-2), a carboxyl carbon at $\delta_C$ 178.6 (C-28), and eight $sp^2$ hybridized carbon signals, implying that the structure of compound **8** was an oleanane-type triterpenoid skeleton attached to a *trans*-feruloyl moiety. Detailed observation of the 1D NMR data disclosed similarities to the spectrum of 23-*trans-p*-coumaroyloxy-2α,3β-dihydroxy-olean-12-en-28-oic acid,[18] and further spectroscopic data analysis of the HSQC

and HMBC spectra (Fig. 2A) showed the apparent differences. The *trans*-feruloyl moiety was attached to C-24, on account of the upfield shift observed for C-23 ($\delta_C$ 22.9) and the downfield shift observed for C-24 ($\delta_C$ 66.4) in the $^{13}$C-NMR spectrum, together with the HMBC correlations (Fig. 2A) of H-24$\alpha$, 24$\beta$ to C-3, C-4 and C-9′. Additionally, significant NOESY correlations (Fig. 2B) were observed from H-2 ($\delta_H$ 3.77) to H-25, demonstrating that H-2 was β-oriented, and the orientation of H-3β of **8** could be deduced from the coupling constant of $J_{H\text{-}2\beta/H\text{-}3\beta}$ = 6.1 Hz and the NOESY correlation of H-3 ($\delta_H$ 3.50) to H-24$\alpha$ and H-24β. Therefore, compound **8** was certified as 24-*O*-*trans*-feruloyl-2α,3α-dihydroxy-olean-12-en-28-oic acid.

Compounds **9** and **10** were isolated as white amorphous powders, and the HRESIMS negative ions at *m*/*z* 647.3955 [M − H]$^-$ and 617.3837 [M − H]$^-$ determined their molecular formulas to be $C_{40}H_{56}O_7$ and $C_{39}H_{54}O_6$, respectively. The NMR data of **9** showed a close similarity to the spectrum of **8**, except for the absence of the hydroxyl group at C-2 in **9**. The 1D NMR spectrum (Table 2) of **9** indicated one oxygenated methine at $\delta_H$ 3.52 (dd, 6.3, 2.7, H-3) and two oxygenated aliphatic carbons at $\delta_C$ 68.5 (C-3) and 66.8 (C-24). In addition, the NMR data of **10** was very similar to that of **9**, except that the *trans*-feruloyl group in **9** was replaced by a *trans*-*p*-coumaroyl group in **10**. Accordingly, compounds **9** and **10** were elucidated to be 24-*O*-*trans*-feruloyl-3α-hydroxy-olean-12-en-28-oic acid and 24-*O*-*trans*-*p*-coumaroyl-3α-hydroxy-olean-12-en-28-oic acid, respectively.

Compound **11** was obtained as a white amorphous powder, and it had the identical molecular formula of $C_{40}H_{56}O_7$ as **9**, and this was established *via* the HRESIMS negative ion at *m*/*z* 647.3942 [M − H]$^-$ (calc. as 647.3948). The NMR data (Table 2) of **11** closely resembled that of **9**, indicating that the planar structures of these compounds were the same. Additionally, the NOESY correlations (Fig. 2B) from H-3 ($\delta_H$ 3.16) to H-5 and H-9, along with the coupling constant of $J_{H\text{-}2\beta/H\text{-}3\alpha}$ = 11.8 Hz demonstrated that H-3 was α-oriented. Consequently, **11** was determined to be 24-*O*-*trans*-feruloyl-3β-hydroxy-olean-12-en-28-oic acid.

The other isolated eight compounds were identified as 3β-*O*-*trans*-caffeoyl-28-hydroxylupane (**5**),[19] betulinic acid 3β-caffeate (**6**),[20] 3β-*O*-*trans*-coumaroyl betulinic acid (**7**),[17] scaphopeta-lumate (**12**),[21] 3β-*O*-(*Z*)-coumaroyl oleanolic acid (**13**),[22] 2α,3β-dihydroxyolean-18-en-28-oic acid (**14**),[23] morolic acid (**15**),[24] and morolic acid 3-*O*-caffeate (**16**)[25] through comparison of their NMR data with the reported spectroscopic data in the references.

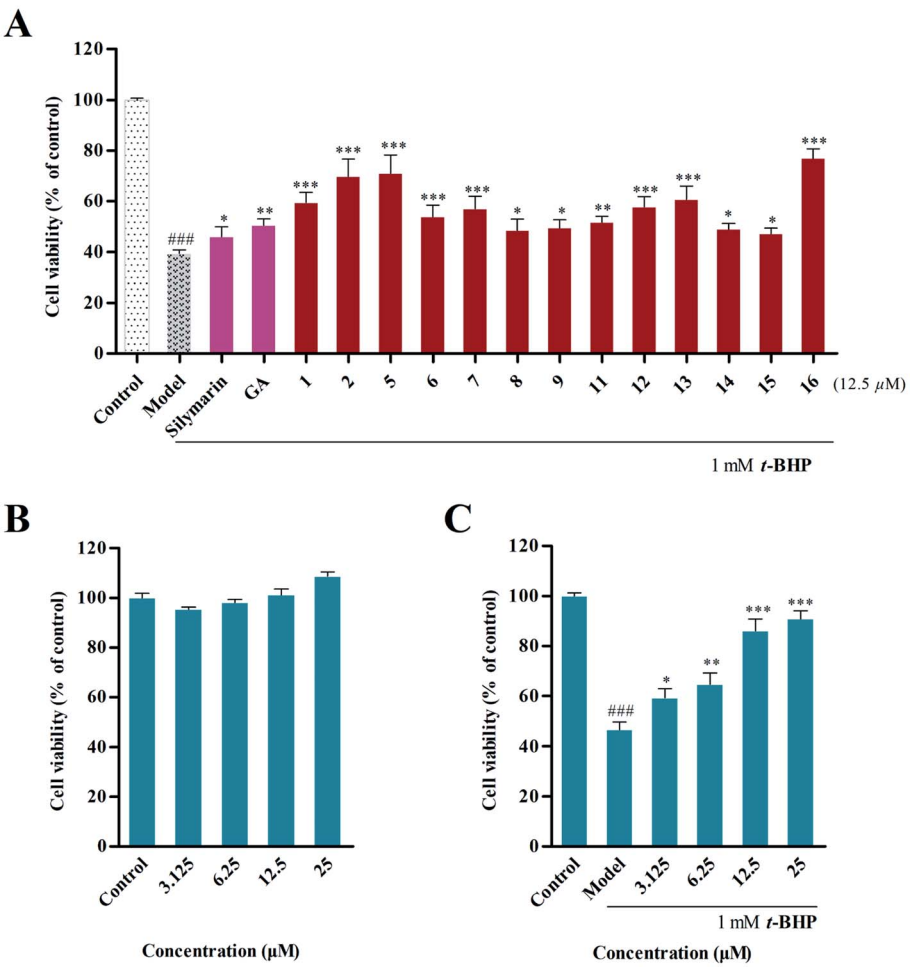


Fig. 3 (A) Evaluation of the hepatoprotective effect of the isolated compounds (12.5 μM) on *t*-BHP-induced hepatotoxicity in HepG2 cells. (B) Cytotoxicity assay of compound **16** against HepG2 cells. (C) Hepatoprotective activity of **16** with concentrations of 3.125, 6.25, 12.5 and 25 μM.

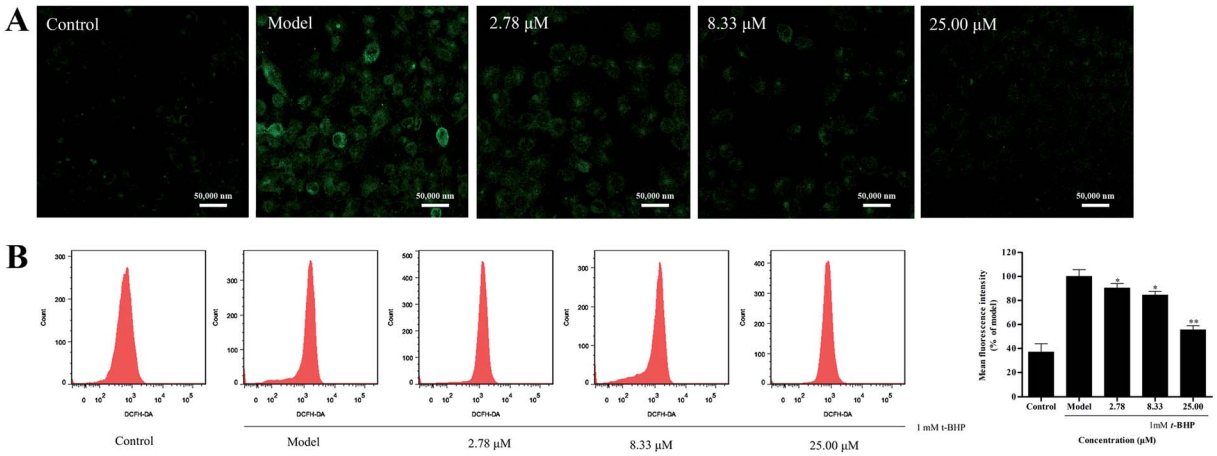


Fig. 4 Effect of compound **16** on the intracellular ROS level of *t*-BHP-induced hepatotoxicity in HepG2 cells, and the intracellular ROS levels were measured by laser scanning confocal microscopy (A) and flow cytometry (B).

### 3.2 Evaluation of hepatoprotective activity

*t*-BHP can be metabolized to harmful free radical intermediates, which are widely used to induce hepatotoxicity in HepG2 cells,[26] and the cell viability can be determined by MTT assay. Thus, the protective effects of the isolated compounds (12.5 μM) on *t*-BHP-induced hepatotoxicity in HepG2 cells were investigated, and silymarin and ammonium glycyrrhetate were used as positive controls. Our results (Fig. 3A) indicated that compounds **2**, **5** and **16** showed potent hepatoprotective activity with increased cell survival rates (CSRs) of 69.81 ± 5.61%, 71.04 ± 5.95% and 77.01 ± 3.05%, respectively, compared with the results of the model group (39.63 ± 1.2%).

Subsequently, the ability of **16** to protect cells from *t*-BHP-induced oxidative injury was further examined. The cytotoxic assay revealed that **16** did not show cytotoxic activity on HepG2 cells at concentrations of 3.125, 6.25, 12.5 and 25 μM (Fig. 3B), and significant hepatoprotective activity was further observed in these concentrations in **16**. In particular, pretreatment of 25 μM of **16** could improve cell survival with a rate of 90.95 ± 3.19%, compared with that of the model group (46.74 ± 2.95%) (Fig. 3C).

### 3.3 Preliminary structure–activity relationship

A preliminary structure–activity relationship of the isolated compounds was determined *in vitro*. Among them, compounds **5** and **16** exhibited the most obvious hepatoprotective activity (CSR = 71.04 ± 5.95% and 77.01 ± 3.05%), and these had the same substitution at C-3, suggesting that the *trans*-caffeoyl moiety possibly plays a positive role in the hepatoprotective activity. Meanwhile, comparison of the activities of **1**, **2**, **5** and **6** indicated that the hydroxymethyl group contributed more to the hepatoprotective activity than the carboxy group that is located at C-28. Furthermore, it was observed that compounds **12** and **13**, which have a *trans-p*-coumaroyl or *trans*-feruloyl group at C-3, displayed more potent effects than compounds **8–9** and **11** that possessed this substituent at C-24, suggesting that different positions of substituent groups may affect their bioactivities. In addition, compound **8**, having an additional α-hydroxyl group at C-2, was

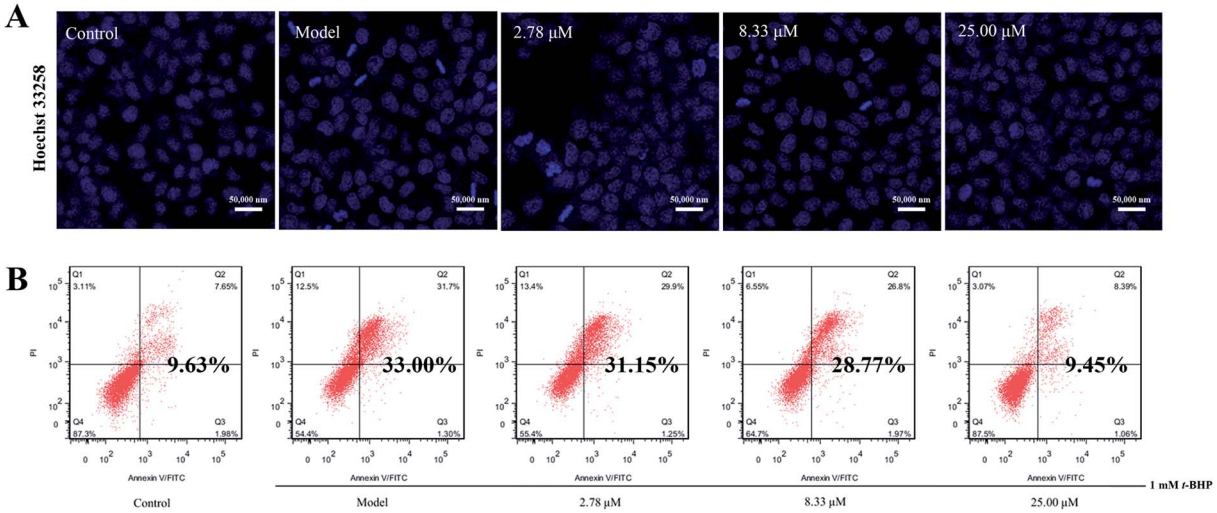


Fig. 5 (A) HepG2 cell nuclei were stained with Hoechst 33258 and imaged using a laser scanning confocal microscope (scale bar 50 μm). (B) Apoptosis rates of *t*-BHP-induced hepatotoxicity in HepG2 cells were detected by annexin V-FITC/PI double staining using flow cytometry.

found to possess similar bioactivity as **9**. This revealed that this hydroxyl group might have few effects on the activity. Additionally, the introduction of a *trans*-caffeoyl moiety resulted in increased activity by comparing the effects of **15** and **16**.

### 3.4 Inhibition of intracellular ROS accumulation

Overproduction of reactive oxygen species (ROS) could induce cellular oxidative damage, which is widely considered as a possible mechanism upstream of *t*-BHP-induced oxidative injury. In the present study, we found that *t*-BHP treatment significantly increased the amount of intracellular ROS compared with the control cells. However, pretreatment with compound **16** (2.78, 8.33, and 25.00 μM) inhibited the over-accumulation of the intracellular ROS level (Fig. 4A). At the same time, quantitative analysis also showed that **16** ameliorated *t*-BHP-induced intracellular ROS accumulation in HepG2 cells in a dose-dependent manner (Fig. 4B).

### 3.5 Suppression effect of *t*-BHP-induced apoptosis

Excessive ROS may cause more extensive and irreparable cell injury, leading to the occurrence of cell death through apoptosis or necrosis.[27] In addition, apoptosis has originally been described as morphological changes, with nuclear condensation and fragmentation being the most recognizable hallmarks. Therefore, we employed Hoechst 33258 staining to observe the morphology of cell nuclei. As illustrated in Fig. 5A, clearly condensed and fragmented cell nuclei were observed when they were treated with *t*-BHP alone, while the pretreatment of compound **16** reduced *t*-BHP-induced cell nuclei shrinkage and fragmentation, compared with that of the model group.

In addition, the apoptosis rate was investigated *via* annexin V-FITC/PI double staining combined with flow cytometry, and the results revealed that *t*-BHP treatment clearly promoted the apoptosis rate from 9.63% for the control to 33.00%. However, pretreatment of **16** at concentrations of 2.78, 8.33, and 25.00 μM decreased the percentage of apoptosis in cells to 31.15%, 28.77% and 9.45%, respectively (Fig. 5B). These findings suggest that **16** suppresses *t*-BHP-induced apoptosis in HepG2 cells.

## 4. Conclusions

In this research, a systemic study to identify and assess the bioactive triterpenoids from the whole plant of *Leptopus chinensis*, in order to investigate their hepatoprotective activities, has been carried out. Ultimately, eight unknown pentacyclic triterpenoids (**1–4** and **8–11**) and eight known analogues (**5–7** and **12–16**) were obtained from this plant for the first time, and they have a common feature where the phenylpropanoid moiety is attached to a triterpenoid skeleton. Compounds **1–4** have an unusual skeleton with the transformation of the 20,29-double bond to a hydroxyl group located at C-20, and **8–11** feature a rare position of the phenylpropanoid moiety attached at C-24, with an α-orientation of the hydroxyl group at C-3. In addition, the *in vitro* measurements discovered that compounds **2**, **5** and **16** display a significant protective effect on *t*-BHP-induced hepatotoxicity in HepG2 cells. Furthermore, **16** markedly ameliorates *t*-BHP-induced intracellular ROS accumulation and cell apoptosis in HepG2 cells. The discovery of these compounds enriches the structural diversity of pentacyclic triterpenoids and provides the potential for plant-derived natural products to be used for hepatoprotective drugs.

## Conflicts of interest

There are no conflicts to declare.

## Acknowledgements

This work was supported by the LiaoNing Revitalization Talents Program (No. XLYC 1905019) and the Natural Science Foundation of Liaoning Province (No. 201602691).

## Notes and references

1 A. H. Zhang, H. Sun and X. J. Wang, *Eur. J. Med. Chem.*, 2013, **63**, 570–577.
2 F. S. Wang, J. G. Fan, Z. Zhang, B. Gao and H. Y. Wang, *Hepatology*, 2014, **60**, 2099–2108.
3 S. Shukla and A. Mehta, *Braz. J. Bot.*, 2015, **38**, 199–210.
4 M. Gordaliza, *Clin. Transl. Oncol.*, 2007, **9**, 767–776.
5 G. B. Xu, Y. H. Xiao, Q. Y. Zhang, M. Zhou and S. G. Liao, *Eur. J. Med. Chem.*, 2018, **145**, 691–716.
6 A. S. Negi, J. K. Kumar, S. Luqman, K. Shanker, M. M. Gupta and S. P. S. Kbanuja, *Med. Res. Rev.*, 2008, **28**, 746–772.
7 J. R. Patel, P. Tripathi, V. Sharma, N. S. Chuhan and V. K. Dixit, *J. Ethnopharmacol.*, 2011, **138**, 286–313.
8 M. I. Ezzat, M. M. Okba, S. H. Ahmed, H. A. EI-Banna, A. Prince, S. O. Mohamed and S. M. Ezzat, *PLoS One*, 2020, **15**, 1–23.
9 J. B. Calixto, A. R. Santos, F. V. Cechinel and R. A. Yunes, *Med. Res. Rev.*, 1998, **18**, 225–258.
10 Editor Committee for Flora of China of Chinese Academy of Science, *Flora of Chin*, Science Press, 1994, vol. 44, p. 19.
11 Y. J. Chen, S. X. Cheng, Y. Long and Q. D. Hou, *J. Zhengzhou Univ., Med. Sci.*, 2008, **43**, 602–603.
12 Z. Y. Wu, *Xinhua Bencao Gangyao*, Shanghai Science and Technology Press, 1991, p. 225.
13 L. B. Qu, X. L. Chen, J. S. Lu, J. W. Yuan and Y. F. Zhao, *Chem. Nat. Compd.*, 2005, **41**, 565–568.
14 J. S. Lu, X. L. Chen, Y. Long, Q. Z. Zhao, L. B. Qu, L. Jia and J. Y. Wei, *Chin. Tradit. Herb. Drugs*, 2001, **32**, 112–113.
15 Y. R. Yang, L. P. Long, X. X. Zhang, K. R. Song, D. Wang, X. Xiong, H. Y. Gao and L. P. Sha, *RSC Adv.*, 2019, **9**, 31758–31772.
16 D. Wang, D. Su, X. Z. Li, D. Liu, R. G. Xi, H. Y. Gao and X. B. Wang, *RSC Adv.*, 2016, **6**, 27434–27446.
17 N. Q. Chien, N. V. Hung, B. D. Santarsiero, A. D. Mesecar, N. M. Cuong, D. D. Soejarto, J. M. Pezzuto, H. H. Fong and G. T. Tan, *J. Nat. Prod.*, 2004, **67**, 994–998.
18 J. Q. Gu, E. J. Park, L. Luyengi, M. E. Hawthorne, R. G. Mehta, N. R. Farnsworth, J. M. Pezzuto and A. D. Kinghorn, *Phytochemistry*, 2001, **58**, 121–127.
19 A. Patra, S. K. Chaudhuri and S. K. Panda, *J. Nat. Prod.*, 1988, **51**, 217–220.

20 H. Pan, L. N. Lundgren and R. Andersson, *Phytochemistry*, 1994, **37**, 795–799.
21 J. C. Vardamides, A. G. B. Azebaze, A. E. Nkengfack, F. R. V. Heerden, Z. T. Fomum, T. M. Ngando, J. Conrad, B. Vogler and W. Kraus, *Phytochemistry*, 2003, **62**, 647–650.
22 H. Takahashi, M. Iuchi, Y. Fujita, H. Minami and Y. Fukuyama, *Phytochemistry*, 1999, **51**, 543–550.
23 J. Zhang, J. Liu, B. Xu, Y. Zhuang, M. Yosikawa and B. C. Yin, *Asian J. Chem.*, 2014, **26**, 4521–4522.
24 J. C. Ferreira Júnior, R. P. L. Lemos and L. M. Conserva, *Biochem. Syst. Ecol.*, 2012, **44**, 208–211.
25 K. J. Park, L. Subedi, S. Y. Kim, S. U. Choi and K. R. Lee, *Bioorg. Chem.*, 2018, **77**, 527–533.
26 T. H. Do, O. Joonseok, M. K. Nguyen, T. D. Trong, V. D. Le, N. Q. D. Thi, M. L. Sang, S. J. Tae, J. Gilsaeng and N. Minkyun, *J. Ethnopharmacol.*, 2013, **150**, 875–885.
27 J. Checa and J. M. Aran, *J. Inflammation Res.*, 2020, **13**, 1057–1073.